Haspin inhibition reveals functional differences of interchromatid axis–localized AURKB and AURKC

Suzanne M. Quartuccio, Shweta S. Dipali, and Karen Schindler*
Department of Genetics, Rutgers, The State University of New Jersey, Piscataway, NJ 08854

ABSTRACT **Aneuploidy is the leading genetic abnormality contributing to infertility, and chromosome segregation errors are common during female mammalian meiosis I (MI). Previous results indicate that haspin kinase regulates resumption of meiosis from prophase arrest, chromosome condensation, and kinetochore–microtubule attachments during early prometaphase of MI. Here we report that haspin inhibition in late prometaphase I causes acceleration of MI, bypass of the spindle assembly checkpoint (SAC), and loss of interchromatid axis–localized Aurora kinase C. Meiotic cells contain a second chromosomal passenger complex (CPC) population, with Aurora kinase B (AURKB) bound to INCENP. Haspin inhibition in oocytes from *Aurkc*$^{-/-}$ mice, where AURKB is the sole CPC kinase, does not alter MI completion timing, and no change in localization of the SAC protein, MAD2, is observed. These data suggest that AURKB on the interchromatid axis is not needed for SAC activation and illustrate a key difference between the functional capacities of the two AURK homologues.**

Monitoring Editor
Kerry S. Bloom
University of North Carolina

Received: Dec 13, 2016
Revised: Jun 16, 2017
Accepted: Jun 20, 2017

INTRODUCTION

Infertility is a common health problem affecting 6.7 million women in the United States and 80 million people worldwide (World Health Organization, 1991). Aneuploidy, or incorrect chromosome numbers in a cell, is the leading genetic abnormality contributing to infertility. Most aneuploid embryos fail to develop, and those born have developmental defects. For unclear reasons, aneuploidy is more common in female than in male germ cells (Jacobs, 1992; Marquez *et al.*, 1998; Volarcik *et al.*, 1998) and can frequently be traced to errors in meiosis I (MI; Angell, 1997; Hassold and Sherman, 2000; Hunt and Hassold, 2002; Kuliev *et al.*, 2011). Therefore it is imperative to investigate how MI chromosome segregation is regulated to understand why errors occur.

One regulator of MI chromosome segregation is haspin kinase (Nguyen *et al.*, 2014). Haspin is an atypical serine/threonine kinase (Higgins, 2003), first identified in mouse spermatocytes (Tanaka *et al.*, 1999), that phosphorylates histone H3 at threonine 3 (H3T3; Dai *et al.*, 2005). In mammalian mitotic cells, phosphorylation of H3T3 recruits Survivin, a member of the chromosomal passenger complex (CPC), which also contains borealin, INCENP, and Aurora kinase B (AURKB), the catalytic subunit, to kinetochores (Dai *et al.*, 2005; Kelly *et al.*, 2010; Wang *et al.*, 2010; Yamagishi *et al.*, 2010). RNA interference or inhibition of haspin leads to chromosome misalignment (Dai *et al.*, 2005), disrupts cohesion between sister chromatids (Dai *et al.*, 2006), and perturbs centromeric localization and activity of AURKB (De Antoni *et al.*, 2012). This loss of localized AURKB activity directly prevents the recruitment of spindle assembly checkpoint (SAC) proteins to kinetochores (Ditchfield *et al.*, 2003; Vigneron *et al.*, 2004; Santaguida *et al.*, 2011) and indirectly disrupts SAC recruitment by preventing destabilization of improper kinetochore–microtubule (K–MT) attachments (De Antoni *et al.*, 2012; Wang *et al.*, 2012).

Haspin-dependent phosphorylation of H3T3 also regulates chromosome segregation in meiotic cells. Haspin inhibition beginning in prophase I delays nuclear envelope breakdown, perturbs chromosome condensation, alters CPC localization along the interchromatid axis (ICA) of MI bivalents (Nguyen *et al.*, 2014; Kang *et al.*, 2015) and prevents clustering of microtubule-organizing centers into a bipolar spindle (Balboula *et al.*, 2016). Inhibition of haspin later in prometaphase I leads to spindle pole fragmentation (Balboula *et al.*, 2016) and accelerates the completion of MI (Wang *et al.*, 2016). Whereas defects in the SAC were attributed to loss of Aurora kinase localization (Wang *et al.*, 2016), formal interrogation of Aurora kinase

This article was published online ahead of print in MBoC in Press (http://www.molbiolcell.org/cgi/doi/10.1091/mbc.E16-12-0850) on June 28, 2017.

The authors declare that they have no conflict of interest.

*Address correspondence to: K. Schindler (schindler@biology.rutgers.edu).

Abbreviations used: 5-Itu, 5-iodotubercidin; ACA, anti-centromere antibody; H3T3, histone H3 at threonine 3; ICA, interchromatid axis; K-MT, kinetochore–microtubule; Met I, metaphase I; Met II, metaphase II; MI, meiosis I; PBE, polar body extrusion; Promet I, prometaphase of meiosis I; PSSC, premature segregation of sister chromatids.

localization upon haspin inhibition later in prometaphase I has not been conducted.

Unlike mitotic cells, mammalian meiotic cells contain two forms of the CPC: one with AURKB as the catalytic subunit and the other with the AURKB homologue Aurora kinase C (AURKC). Because ectopically expressed AURKC can support cell division in the absence of AURKB in mitotic cells (Sasai *et al.*, 2004; Slattery *et al.*, 2009) and *Aurkc* expression is enriched in germ cells (Yanai *et al.*, 1997; Tseng *et al.*, 1998), AURKC function was initially interpreted as the meiosis-specific isoform of AURKB. The kinase homologues have functional similarities, and AURKB can compensate for the loss of AURKC because mice lacking *Aurkc* are not infertile (Schindler *et al.*, 2012) and the CPC is still active (Balboula and Schindler, 2014). However, recent evidence suggests that AURKC and AURKB have some nonoverlapping functions in oocytes from wild-type (WT) mice. First, the kinases have distinct localization patterns: AURKC localizes to the ICA of MI bivalents, whereas AURKB localizes to the spindle (Balboula and Schindler, 2014). Second, different phenotypes are observed when both AURKB and AURKC are inhibited compared with AURKC inhibition alone. Experiments using dominant-negative AURKC, which disrupts both AURKB and AURKC activity (Chen *et al.*, 2005; Balboula and Schindler, 2014), or treatment with pan-Aurora inhibitor ZM447439 led to bypass of the SAC (Lane *et al.*, 2010). In contrast, inhibition of AURKC alone, using an *Aurkc* dominant-negative allele that does not inhibit AURKB, causes metaphase I (Met I) arrest and does not perturb SAC function (Balboula and Schindler, 2014). Finally, overexpression of AURKC leads to activation of the anaphase-promoting complex/cyclosome (APC/C) and cell cycle progression, whereas overexpression of AURKB fails to activate the APC/C (Sharif *et al.*, 2010).

RESULTS AND DISCUSSION

Haspin delays anaphase onset to ensure proper chromosome segregation

Haspin phosphorylation of H3T3 (H3pT3) in oocytes is critical for meiotic resumption, chromosome condensation, and CPC localization. These functions were established by inhibiting haspin in either prophase I or early prometaphase I (Promet I), just after nuclear envelope breakdown (Nguyen *et al.*, 2014). Because protein kinases often have temporally distinct functions in cell cycles, we hypothesized that haspin would also have functions later in Promet I, after chromosome condensation has occurred but before chromosome alignment.

To determine whether haspin functions in late Promet I, prophase-I–arrested oocytes were matured in vitro for 5 h before addition of 0.5 μM 5-iodotubercidin (5-Itu) or vehicle as a control (100% ethanol [EtOH]) to the maturation medium. This acute inhibition of haspin is effective because H3pT3 was lost when examined 2.5 h later, compared with controls (Figure 1A). We also note that unlike haspin perturbation in early Promet I (Nguyen *et al.*, 2014), haspin inhibition in late Promet I did not alter DNA morphology. Live-imaging analysis revealed that when haspin was inhibited in late Promet I, oocytes exhibited 3-h acceleration in MI completion, as monitored by polar body extrusion (PBE; Figure 1, B and C). On average, controls extruded a polar body 13.7 h after maturation induction, whereas 5-Itu–treated oocytes extruded a polar body after 10.6 h. These altered MI kinetics agree with recent work showing that haspin inhibition late in Promet I leads to premature anaphase onset (Wang *et al.*, 2016). This accelerated completion of meiosis is the opposite of the delay in meiotic progression phenotype reported previously (Nguyen *et al.*, 2014) and shown here (17.9 h; Figure 1, B and C) when haspin is inhibited in prophase I.

The opposing changes in MI kinetics based on timing of haspin inhibition provide evidence for distinct temporal haspin functions during MI. Haspin could act on different substrates throughout Promet I, or accumulation of the AURKB/C antagonist protein phosphatase 2A (Yoshida *et al.*, 2015) could make recruitment of Aurora kinase by haspin in late Promet I critical to prevent premature anaphase onset. Further studies are needed to better understand this temporally regulated balance of kinase/phosphatase activity in late Promet I.

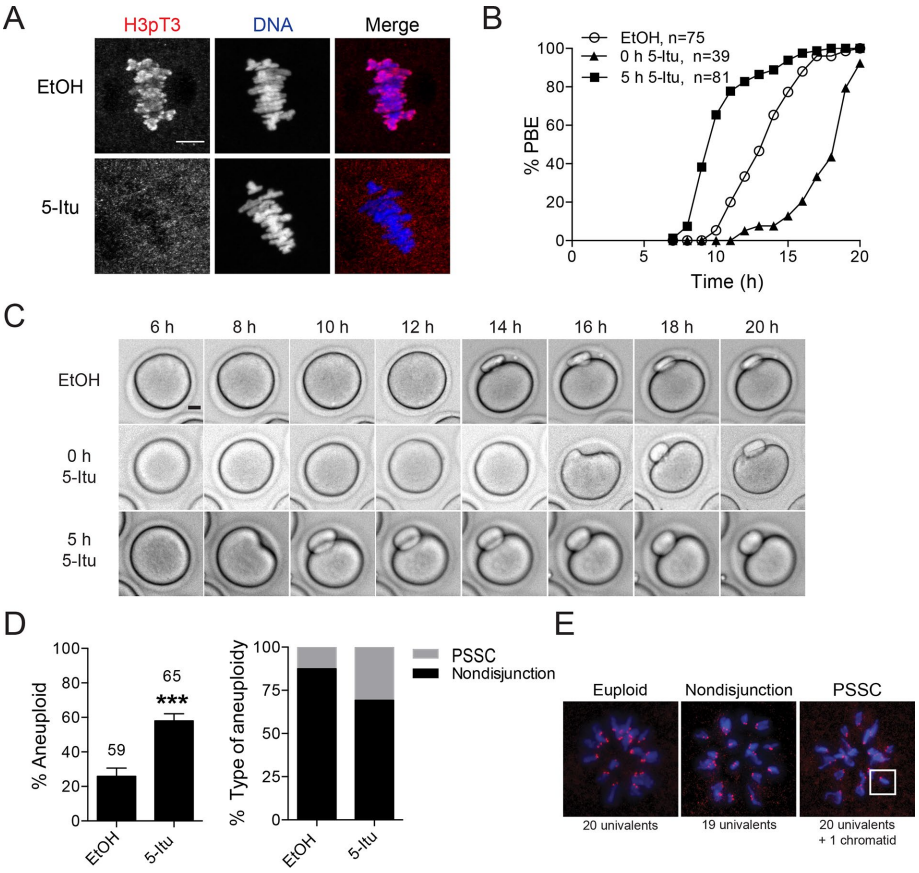

FIGURE 1: Haspin inhibition during late prometaphase I accelerates MI and increases aneuploidy. (A) Representative *z*-projections of phosphorylated histone 3 at threonine 3 (H3pT3; red) and DNA (blue) at Met I (7.5 h) after treatment with EtOH or 0.5 μM 5-Itu at late Promet I (5 h). (B) Timing of PBE for oocytes matured in vitro. (C) Representative images of oocytes at the indicated time after meiotic resumption. (D) Percentage of aneuploid oocytes. ***$p = 0.0009$. Aneuploid oocytes further analyzed for PSSC or nondisjunction errors. n.s., two-way analysis of variance. (E) Representative *z*-projections of each phenotype. DNA (blue) and kinetochores (ACA; red). Data are mean ± SEM. Bar, 10 μm.

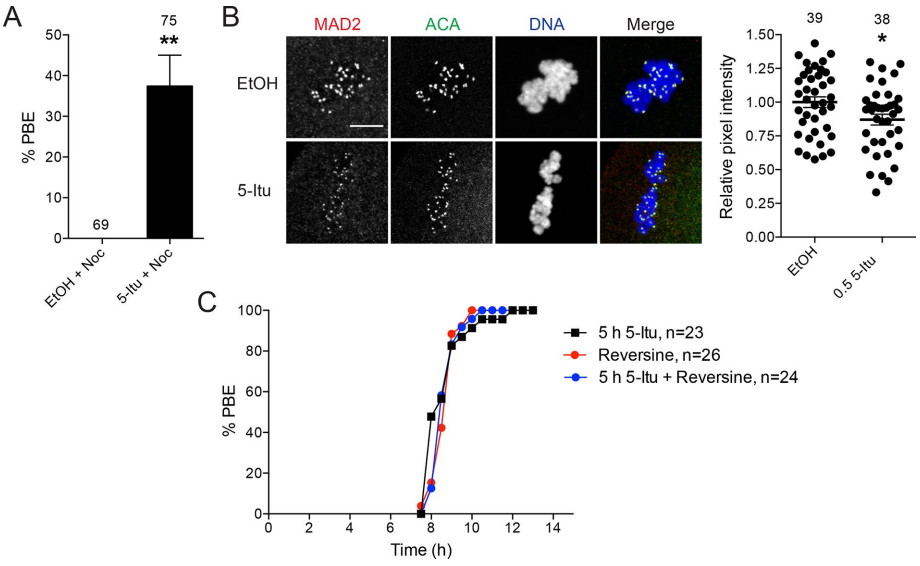

FIGURE 2: Perturbation of haspin hinders SAC response. (A) Percentage of oocytes extruding polar body after treatment with EtOH or 0.5 µM 5-Itu and 5 µM nocodazole (Noc) at late Promet I (5 h). (B) Representative *z*-projections of oocytes treated with 400 nM Noc, 5 µM MG132, and EtOH or 0.5 µM 5-Itu at late Promet I and matured to 9 h. MAD2 (red), ACA (green), and DNA (blue). Quantification of MAD2 levels (right); each dot is the average intensity of an oocyte. (C) Timing of PBE for oocytes matured in vitro with 0.5 µM 5-Itu, 1.0 µM reversine, or 0.5 µM 5-Itu and 1.0 µM reversine added at 5 h. Data are mean ± SEM. $^{**}p = 0.0026$, $^{*}p = 0.0231$. Bar, 10 µm.

Meiosis is a regulated developmental process, and alterations in cell-cycle kinetics could compromise egg quality (Holt *et al.*, 2012). To determine the consequences of altered cell-cycle kinetics, we performed in situ chromosome counting analyses on in vitro–matured metaphase II (Met II) eggs. Control oocytes produced some aneuploid eggs (25.8%; Figure 1D), whereas inhibition of haspin activity significantly increased the percentage of aneuploid eggs at Met II (58.0%; Figure 1D). The aneuploid eggs were further analyzed to determine whether the error resulted from nondisjunction or premature segregation of sister chromatids (PSSC) by counting individual kinetochores labeled with anti-centromere antibody (ACA; Figure 1E). Nondisjunction occurred more frequently in both EtOH- and 5-Itu–treated eggs compared with PSSC. An increase in the incidence of PSSC was observed in 5-Itu–treated eggs (25.9%) compared with EtOH-treated eggs (12.5%); however, this was not statistically significant. These errors were likely due to insufficient time to correct improper attachments (bivalents undergo an average of three error corrections before biorienting; Kitajima *et al.*, 2011). These data demonstrate that haspin activity is needed in late Promet I to prevent premature entry into anaphase.

Haspin is required to maintain the SAC in late prometaphase I

The acceleration of MI completion observed in haspin-inhibited oocytes phenocopies the loss of SAC components (Wassmann *et al.*, 2003; Homer *et al.*, 2005; Niault *et al.*, 2007; McGuinness *et al.*, 2009; Hached *et al.*, 2011). To examine SAC integrity, we treated control and 5-Itu–treated oocytes with nocodazole (5 µM) to depolymerize the microtubules in late Promet I (5 h). The oocytes were then matured and imaged live for an additional 15 h to monitor completion of MI via PBE, a measure that the SAC failed to induce a Met I arrest. We note that oocytes that lack a functional SAC can extrude a PB without microtubules. No control oocytes treated with EtOH and nocodazole extruded a polar body, indicating intact SAC response. However, when nocodazole was combined with 5-Itu treatment late in Promet I, 37.5% of oocytes extruded a polar body (Figure 2A), providing evidence for a weakened SAC response.

To confirm the weakened SAC response, we quantified the intensity of MAD2, a SAC component, staining at the kinetochores. The amount of MAD2 localized at kinetochores correlates with SAC activity (Collin *et al.*, 2013). Because SAC component levels are weak or undetectable in oocytes at Met I (Wang *et al.*, 2016), we added nocodazole (400 nM) to the culture medium in addition to EtOH or 5-Itu at late Promet I (5 h). This strategy established a sensitized system to assess small but significant changes in MAD2 recruitment. Finally, to prevent oocytes from progressing to anaphase I, 5 µM MG132, a proteasome inhibitor, was added, and oocytes were matured for a total of 9 h. Although there was oocyte-to-oocyte variability, 5-Itu–treated oocytes exhibited a 13% decrease in MAD2 immunoreactivity at kinetochores compared with controls (Figure 2B). Of note, small numbers of misaligned chromosomes are not sufficient to inhibit APC/C in oocytes (Lane and Jones, 2014). The oocytes with the lowest MAD2 intensity (Figure 2B) were likely the oocytes that would bypass the SAC.

Further confirmation of a weakened SAC was measured by treating oocytes with 1.0 µM MPS1 inhibitor reversine in late Promet I (5 h). Inhibition of MPS1 blocks recruitment of SAC proteins (Santaguida *et al.*, 2010; Hiruma *et al.*, 2016). Live-cell imaging revealed an average PBE timing of 8.8 h in reversine-treated oocytes, which was not significantly different from that in 5-Itu–treated oocytes (8.8 h). Combining reversine and 5-Itu treatments did not cause an additive effect, indicating that both 5-Itu and reversine affect the same pathway.

Haspin inhibition disrupts AURKC localization and activity at the ICA in late Promet I

H3T3 phosphorylation by haspin recruits the CPC to chromosomes, which activates the SAC and destabilizes improper K-MT attachments (Dai *et al.*, 2005; Wang *et al.*, 2010, 2012; De Antoni *et al.*, 2012). Because inhibition of haspin early in Promet I (0 and 2 h after meiotic resumption; De Antoni *et al.*, 2012) specifically perturbs ICA-localized AURKC, we asked whether haspin inhibition late in Promet I had a similar effect and therefore caused defects in SAC activity.

To answer this question, we matured prophase-I–arrested oocytes for 5 h before inhibiting haspin. After fixation at Met I (7.5 h after maturation induction), we quantified the amount of chromosome-localized AURKC by immunocytochemistry. The 5-Itu–treated oocytes showed a significant decrease (60%) in localized AURKC compared with control oocytes (Figure 3, A–C). This reduction in AURKC is similar to the reduction observed when oocytes were treated with 5-Itu in prophase I or early Promet I (Nguyen *et al.*, 2014). Altered localization of the CPC was confirmed by quantifying the amount of chromosome-localized Survivin by immunocytochemistry. The 5-Itu–treated oocytes similarly showed a significant reduction (57%) in localized Survivin compared with controls (Figure 3, D–F).

To assess localized activity of AURKC, we measured the signal intensity of phosphorylated INCENP (pINCENP). Oocytes were

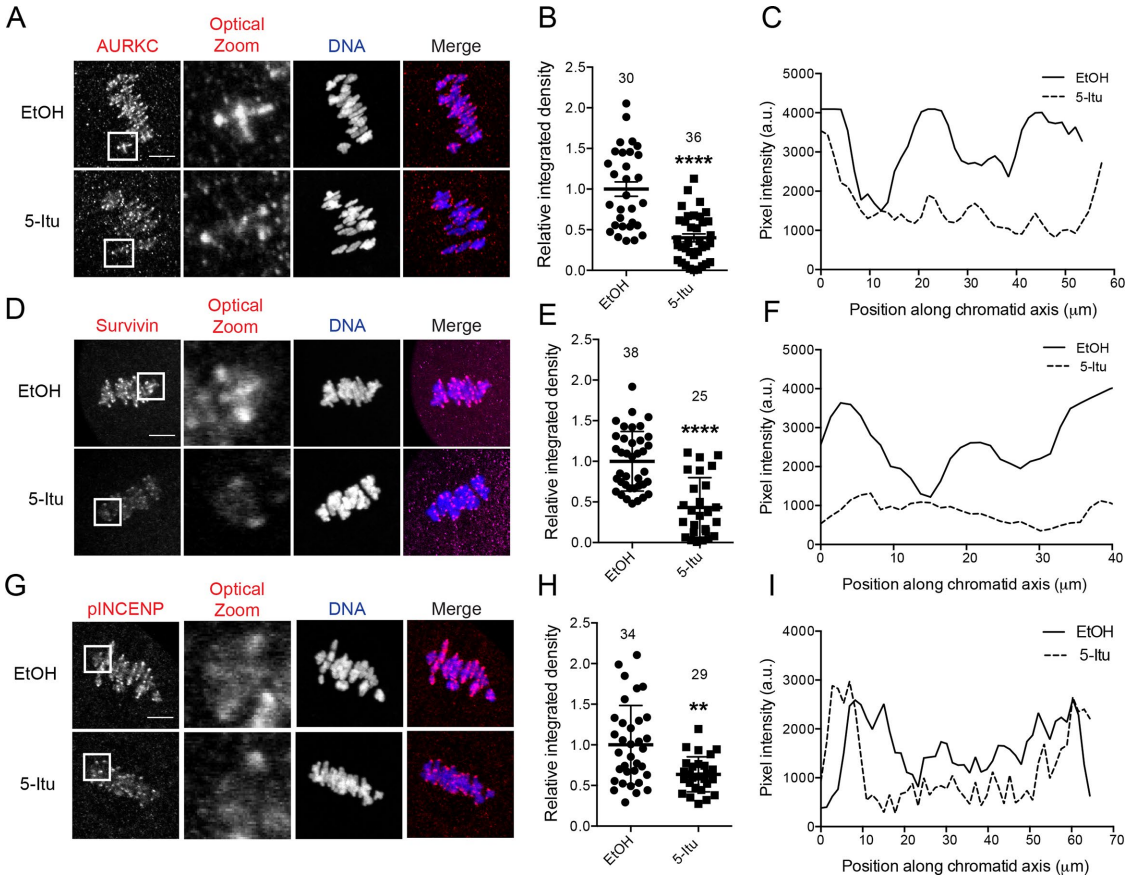

FIGURE 3: Inhibition of haspin during late Promet I disrupts CPC localization and activity at the ICA. Representative z-projections of AURKC (red; A), Survivin (red; D), or phosphorylated INCENP (pINCENP, red; G) and DNA (blue) after treatment with either EtOH or 0.5 μM 5-Itu at late Promet I (5 h). Zoomed images show the bivalent indicated in the box from an optical slice. (B, E, H) Chromosome intensity of AURKC, Survivin, or pINCENP. (C, F, I) Quantitative assessment of chromosome image in zoom using "plot profile" function in ImageJ. Data show mean ± SEM. ****$p < 0.0001$, **$p = 0.0016$. Bar, 10 μm.

treated with EtOH or 5-Itu at late Promet I and matured to Met I before fixation. The 5-Itu–treated oocytes exhibited a 33% decrease in pINCENP signal on chromosomes compared with controls (Figure 3, G–I). These data are similar to those reported when haspin was inhibited in prophase I or early Promet I (Nguyen *et al.*, 2014) and demonstrate that localization and activity of AURKC at the ICA are dynamic processes requiring haspin activity throughout Promet I.

We showed that 5-Itu effectively eliminates H3pT3 localization on the ICA and at the kinetochores (Figure 1A), and yet AURKC, Survivin, and pINCENP localizations persist at kinetochores in 5-Itu–treated oocytes (Figure 3, C, F, and I). These results differ from the loss of AURKB localization at kinetochores observed in mitotic cells after Haspin inhibition (De Antoni *et al.*, 2012). The CPC may localize to the kinetochores in oocytes in an H3pT3-independent manner similar to BUB1-mediated phosphorylation of histone 2A at threonine 120 (Yamagishi *et al.*, 2010). Alternatively, haspin itself at kinetochores may recruit the CPC in meiotic cells. Regardless of mechanism to recruit CPC components to kinetochores, this localization is not sufficient for SAC activation in WT oocytes.

Haspin inhibition does not perturb SAC activity in *Aurkc*$^{-/-}$ mice

Oocytes contain both AURKB and AURKC-bound CPC. Because haspin regulates AURKB-CPC localization in mitotic cells, we wondered whether haspin also regulates AURKB-CPC in oocytes. AURKB localizes to the ICA and kinetochores in the absence of AURKC and becomes the catalytic subunit of the CPC (Schindler *et al.*, 2012; Balboula and Schindler, 2014). To evaluate this regulatory pathway, we inhibited haspin in prophase I and late Promet I oocytes isolated from *Aurkc*$^{-/-}$ mice. Immunocytochemical analysis of oocytes showed loss of H3pT3 on chromosomes (Figure 4A) 2.5 h after 5-Itu treatment. CPC localization was analyzed through measurement of Survivin immunostaining. Oocytes treated with 5-Itu in late Promet I exhibited less (43% reduction) Survivin staining than did controls (Figure 4B). AURKB localization could not be measured due to lack of a reliable antibody; however, AURKB activity was analyzed by measuring pINCENP. A 33% decrease in pINCENP was measured in haspin-inhibited *Aurkc*$^{-/-}$ oocytes compared with controls (Figure 4C). These results indicate that H3pT3 regulates AURKB-CPC localization along chromosome arms similar to AURKC in WT oocytes (Figures 1A, 3B, and C).

To our surprise, haspin-inhibited oocytes from *Aurkc*$^{-/-}$ mice displayed similar PBE kinetics to *Aurkc*$^{-/-}$ oocytes treated with EtOH (Figure 4, D and E). Control-treated *Aurkc*$^{-/-}$ oocytes exhibit a ~3-h delay in PBE (16.2 h) compared with WT oocytes, and a proportion failed to extrude a polar body, as previously reported (Schindler *et al.*, 2012). One explanation for this observation is that *Aurkc*$^{-/-}$ oocytes have increased checkpoint activity; however, this model has not been formally tested. PBE timing was not significantly altered upon haspin inhibition at either 0 h (15.9 h) or 5 h (14.9 h). The lack of change in PBE timing suggests that haspin-inhibited *Aurkc*$^{-/-}$ oocytes have an intact SAC. To test the integrity of the SAC, we treated *Aurkc*$^{-/-}$

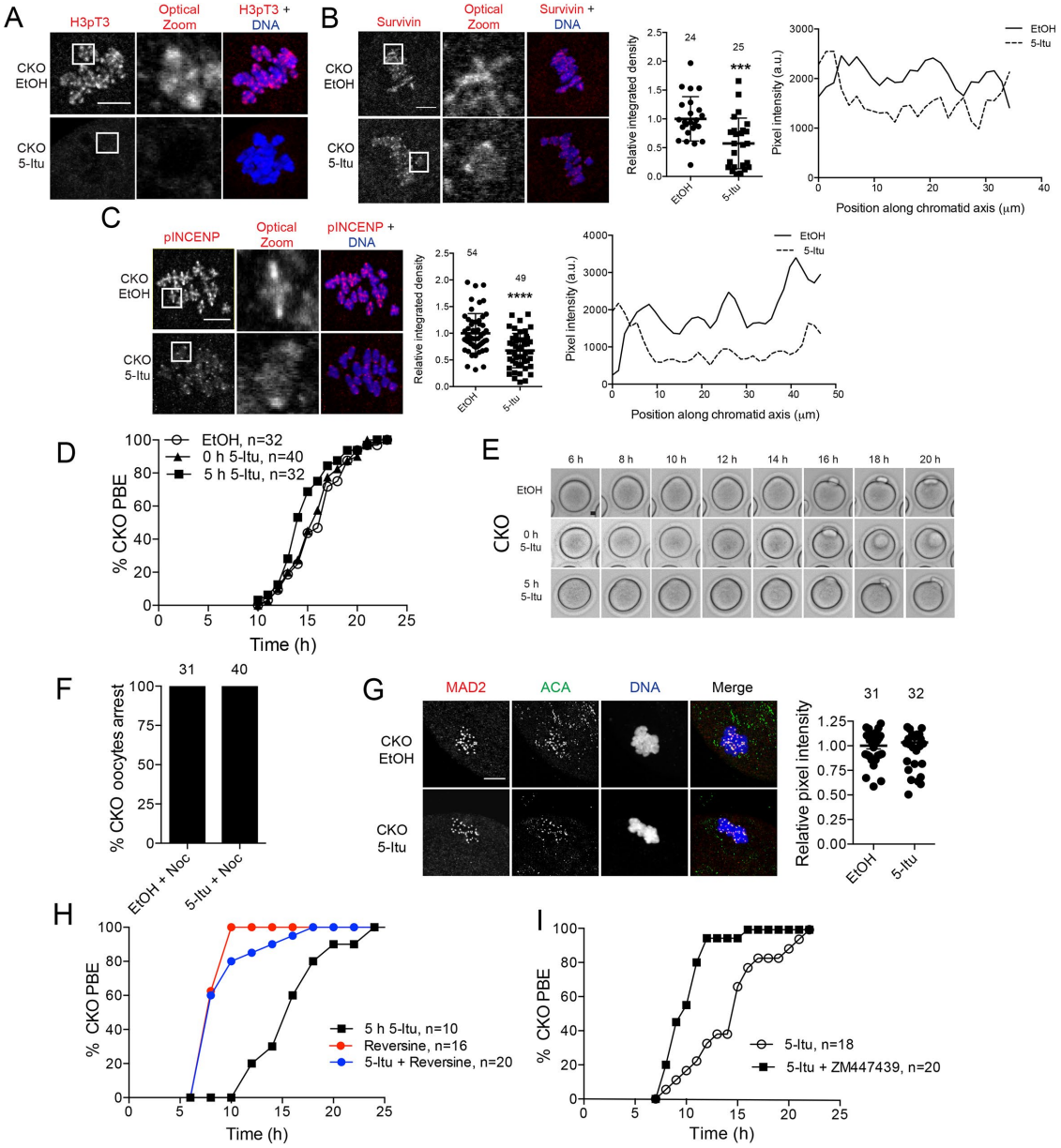

FIGURE 4: *Aurkc*$^{-/-}$ oocytes are not affected by haspin inhibition. (A) Representative *z*-projections of phosphorylated histone 3 at threonine 3 (H3pT3; red) and DNA (blue) in *Aurkc*$^{-/-}$ oocytes at Met I (7.5 h) after treatment with either EtOH or 0.5 μM 5-Itu at late Promet I (5 h). (B) Representative *z*-projections of Survivin (red) and DNA (blue) in *Aurkc*$^{-/-}$ oocytes after treatment with either EtOH or 0.5 μM 5-Itu at late Promet I. Chromosome intensity of Survivin and "plot profile" of chromosome image in zoom. (C) Representative *z*-projections of phosphorylated INCENP (pINCENP, red) and DNA (blue) in *Aurkc*$^{-/-}$ oocytes after treatment with either EtOH or 0.5 μM 5-Itu at late Promet I. Chromosome intensity of pINCENP and "plot profile" of chromosome image in zoom. (D) Timing of PBE for *Aurkc*$^{-/-}$ oocytes matured in vitro with EtOH, 0.5 μM 5-Itu at 0 h, or 0.5 μM 5-Itu at 5 h. (E) Representative images of oocytes at the indicated time after meiotic resumption. (F) Percentage of *Aurkc*$^{-/-}$ oocytes arresting in Met I after treatment with EtOH or 0.5 μM 5-Itu and 5 μM nocodazole (Noc) at late Promet I. (G) Representative *z*-projections of *Aurkc*$^{-/-}$ oocytes treated with 400 nM Noc, 5 μM MG132, and EtOH or 0.5 μM 5-Itu at late Promet I and matured to 9 h. MAD2 (red), ACA (green), and DNA (blue). Quantification of MAD2 levels (right); each dot is the average intensity of an oocyte. (H) Timing of PBE for oocytes matured in vitro with 0.5 μM 5-Itu, 1.0 μM reversine, or 0.5 μM 5-Itu and 1.0 μM reversine at 5 h. (I) Timing of PBE for *Aurkc*$^{-/-}$ oocytes matured in vitro with 0.5 μM 5-Itu or 0.5 μM 5-Itu and 0.5 μM ZM447439 at 5 h. The zoomed images show the chromosome indicated in a box from an optical slice. Data are mean ± SEM. ***$p = 0.0008$, ****$p < 0.0001$. Bar, 10 μm.

oocytes with nocodazole. All haspin-inhibited *Aurkc*$^{-/-}$ oocytes arrested at Met I, demonstrating an intact checkpoint (Figure 4F). To confirm this observation of an intact SAC, we measured MAD2 intensity after treating oocytes with nocodazole (400 nM). Oocytes were fixed 9 h after induction of maturation and analyzed using immunocytochemistry. No difference in MAD2 intensity was measured between EtOH- and 5-Itu–treated oocytes (Figure 4G), suggesting that ICA-localized AURKB-CPC does not regulate SAC activity in meiosis I.

The failure to alter PBE in 5-Itu-treated *Aurkc*$^{-/-}$ oocytes could be due to defects in the APC/C rather than intact SAC activity. To test the integrity of the APC/C, we treated *Aurkc*$^{-/-}$ oocytes with reversine in late Promet I. When SAC recruitment was disrupted in the reversine-treated oocytes, PBE was accelerated (8.9 h) compared with 5-Itu–treated oocytes (16.6 h; Figure 4H). MPS1 inhibition combined with haspin inhibition also accelerated PBE (9.9 h; Figure 4H). These data provide evidence that the APC/C is functional in *Aurkc*$^{-/-}$ oocytes.

To confirm that the activity of AURKB is responsible for the SAC recruitment and PBE timing in *Aurkc*$^{-/-}$ oocytes, we treated *Aurkc*$^{-/-}$ oocytes with the AURKB inhibitor ZM447439. When AURKB is inhibited in the presence of 5-Itu, PBE accelerated (10.1 h) compared with oocytes treated with 5-Itu alone (14.5 h; Figure 4I).

The differences in phenotypes observed after haspin inhibition in WT and *Aurkc*$^{-/-}$ oocytes suggest that AURKB and AURKC regulate SAC activation through different localized populations. AURKB-CPC localized along the ICA is not needed for SAC activation because 5-Itu–treated oocytes from *Aurkc*$^{-/-}$ mice have an intact SAC. In contrast, WT oocytes (containing both AURKB and AURKC) treated with 5-Itu show a decreased recruitment of SAC components and undergo premature anaphase I when ICA-localized AURKC localization is perturbed. AURKB localizes with microtubules of meiotic spindles (Balboula and Schindler, 2014) and likely comes into close proximity to kinetochores and can regulate recruitment of SAC components like MAD2 (Figure 5). When both AURKs are present, AURKC may suppress or displace AURKB activation of the SAC, as previously seen in mitotic cells with overexpression of AURKC, resulting in reduced CPC expression and weakened AURKB activity (Lin *et al.*, 2014). Only in the absence of AURKC can AURKB activate the SAC (Figure 5). It is unclear why kinetochore-localized AURKC would be unable to activate the SAC and why AURKB can, but this finding agrees with the observation that AURKC localized at kinetochores is inactivated at Met I (Rattani *et al.*, 2013). Because there are differences between these two kinases in their ability to autoactivate (Sasai *et al.*, 2016), it is feasible that differences exist in their ability to be inhibited.

This study expands our knowledge of the function of haspin in meiotic cells and how meiotic regulation of the SAC differs from that in mitosis. We show that haspin is critical in late Promet I to delay anaphase onset through positive regulation of the SAC by AURKC. Through haspin inhibition experiments, we also exposed a functional difference in SAC regulation between AURKB- and AURKC-bound CPC. These findings are particularly significant in light of developing cancer therapeutics, which target epigenetic marks to control cell growth. For instance, a tumor overexpressing AURKB could respond differently than one expressing both AURKB and AURKC. Although known to compensate for one another, nonoverlapping functions exist (Sharif *et al.*, 2010; Balboula and Schindler, 2014), and more studies are warranted to better understand the roles of the AURKs in meiotic and mitotic cells.

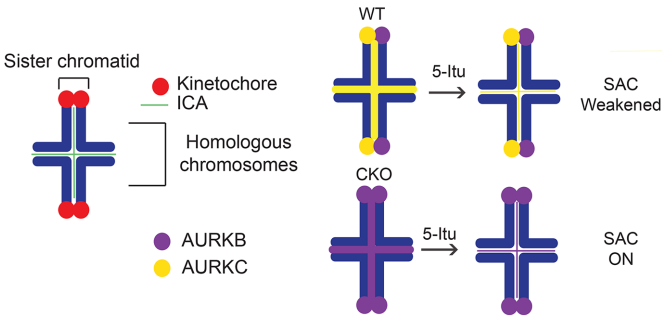

FIGURE 5: Schematic of differential function of interchromatid axis–localized AURKB and AURKC CPC.

MATERIALS AND METHODS

Oocyte collection and maturation

Sexually mature CF-1 (Envigo, Indianapolis, IN) or *Aurkc*$^{-/-}$ female mice (6–12 wk; Kimmins *et al.*, 2007; Schindler *et al.*, 2012) were hormonally primed with 5 IU of equine gonadotropin (EMD Millipore, Billerica, MA) via intraperitoneal injection 48 h before collection in MEM/ polyvinylpyrrolidone with 2.5 μM milrinone (M4659; Sigma-Aldrich, St. Louis, MO). Germinal-vesicle-intact oocytes were isolated and matured in Chatot, Ziomek, Bavister (CZB) medium without milrinone at 37°C in a 5% CO_2, humidified incubator. After 2 h of maturation, oocytes failing to undergo nuclear envelope breakdown were discarded. 5-Itu (10010375; Cayman Chemical, Ann Arbor, MI) was dissolved in 100% ethanol and diluted in CZB at 1:1000. To inhibit proteasome activity, MG132 (474791; EMD Millipore) dissolved in dimethyl sulfoxide (DMSO) was added to the culture medium to a final concentration of 5 μM. To depolymerize microtubules and activate the SAC, nocodazole (487928; Sigma-Aldrich) dissolved in DMSO was added to CZB culture medium to 5 μM or 400 nM as indicated in the figure legends. Reversine (10004412; Cayman Chemical) and ZM447439 (2458; Tocris, Minneapolis, MN) were dissolved in DMSO and added to the culture medium to final concentrations of 1 and 5 μM, respectively. Details for genotyping *Aurkc*$^{-/-}$ mice were described previously (Kimmins *et al.*, 2007; Schindler *et al.*, 2012). All animal experiments were approved by the institutional Animal Use and Care Committee (11-032) and consistent with National Institutes of Health guidelines.

In situ chromosome counting

Chromosome counts were performed as previously described (Duncan *et al.*, 2009; Stein and Schindler, 2011). Briefly, 100 μM monastrol (M8515; Sigma-Aldrich) treatment was added to Met II–arrested eggs for 2 h, 15 min in CZB medium. Eggs were fixed in 2% paraformaldehyde (PFA) and stained with ACA to mark kinetochores and 4′, 6-diamidino-2-phenylindole dihydrochloride (DAPI) to stain DNA. Images captured on Zeiss Axiovert 200M epifluorescence microscope were blinded, and individual kinetochores were counted using ImageJ software (National Institutes of Health, Bethesda, MD).

Immunocytochemistry

After meiotic maturation, oocytes were fixed in phosphate-buffered saline (PBS) containing 2% PFA for 20 min at room temperature for detection of AURKC, ACA, H3pT3, and pINCENP. For detection of MAD2, oocytes were fixed in 3.7% PFA containing 0.1% Triton X-100 for 1 h at room temperature. For detection of Survivin, oocytes were fixed in 4% PFA containing 0.1% Triton X-100 for 30 min at room temperature. Fixed oocytes were stored in blocking buffer (PBS plus 0.3% [wt/vol] bovine serum albumin [BSA] plus 0.01% [vol/vol] Tween-20) at 4°C until processed for immunodetection. After 20 min in permeabilization solution (PBS plus 0.3% [wt/vol] BSA plus 0.1% [vol/vol] Triton X-100), oocytes were incubated in primary antibody diluted in blocking buffer for 1 h at room temperature. After washing, oocytes were incubated in secondary antibody for 1 h at room temperature. After washes, oocytes were mounted in 5 μl of Vectashield containing DAPI (D1306; Life Technologies, Grand Island, NY).

The following antibodies were used for immunofluorescence: AURKC (1:500; A300-BL1217; Bethyl, Montgomery, TX), ACA (1:30; 15-234; Antibodies Incorporated, Davis, CA), H3pT3 (1:100; 39153;

Active Motif, Carlsbad, CA), MAD2 (1:1000; PRB-452C; Biolegend, San Diego, CA), pINCENP (1:1000; M. Lampson, University of Pennsylvania), and Survivin (1:500; 2808; Cell Signaling Technology, Danvers, MA). Secondary antibodies were obtained from Life Technologies and used at 1:200: Alexa Fluor 568 donkey anti-rabbit (A10042) and Alexa Fluor 633 goat anti-human (A21091).

Imaging and image analysis

Fluorescence was detected on a Zeiss 510 Meta laser-scanning confocal microscope under a 40×/1.20 objective. For live imaging, oocytes were transferred into a 96-well dish containing CZB medium. Bright-field image acquisition was started in late Promet I (5 h) using an EVOS FL Auto Imaging System (Life Technologies) with a 10× objective. The EVOS on-stage incubator was maintained at 37°C and 5% CO_2. Images were acquired every 20 min. Note that despite extensive optimization, the live-imaging procedure causes a mild delay (1.5 h) in PBE in controls compared with oocytes matured in the absence of imaging. This delay is likely due to a lack of an oil overlay that is better at maintaining constant CO_2 levels. This condition is important, however, to prevent partitioning of the inhibitor into the oil.

All images were analyzed using ImageJ software. AURKC and Survivin integrated density was determined from maximum *z* projections, with threshold levels set to EtOH control. The integrated density is the product of the area and mean pixel intensity. pINCENP integrated density measurements were taken from middle single slice of the *z*-stack, where the majority of chromosomes were scanned. MAD2 intensity was determined through region of interest measurements taken with ACA as a mask on 20 kinetochores in each oocyte. The average intensity for each oocyte was calculated from the 20 measurements. Relative pixel intensity was determined by dividing average intensity by the average intensity of all EtOH-treated oocytes in the experiment. The pixel intensity of CPC intensity in individual bivalents was produced by drawing a line between ACA foci and using the "plot profiles" function in ImageJ.

Statistical analysis

Unless otherwise indicated, Student's *t* test was used to evaluate the difference between groups using GraphPad Prism software (La Jolla, CA). The differences of $p < 0.05$ were considered significant. All experiments were conducted two to five times, and total oocyte numbers used are indicated on the figures.

ACKNOWLEDGMENTS

We thank Michael Lampson (University of Pennsylvania) for the pINCENP antibody. We also thank Schindler and McKim lab members for their feedback. This work is supported by National Institutes of Health Grants R01-GM112801 and P30 CA072720 to K.S. and K12-GM093854 to S.Q.

REFERENCES

Angell R (1997). First-meiotic-division nondisjunction in human oocytes. Am J Hum Genet 61, 23–32.

Balboula AZ, Nguyen AL, Gentilello AS, Quartuccio SM, Drutovic D, Solc P, Schindler K (2016). Haspin kinase regulates microtubule-organizing center clustering and stability through Aurora kinase C in mouse oocytes. J Cell Sci 129, 3648–3660.

Balboula AZ, Schindler K (2014). Selective disruption of aurora C kinase reveals distinct functions from aurora B kinase during meiosis in mouse oocytes. PLoS Genet 10, e1004194.

Chen HL, Tang CJ, Chen CY, Tang TK (2005). Overexpression of an Aurora-C kinase-deficient mutant disrupts the Aurora-B/INCENP complex and induces polyploidy. J Biomed Sci 12, 297–310.

Collin P, Nashchekina O, Walker R, Pines J (2013). The spindle assembly checkpoint works like a rheostat rather than a toggle switch. Nat Cell Biol 15, 1378–1385.

Dai J, Sullivan BA, Higgins JM (2006). Regulation of mitotic chromosome cohesion by Haspin and Aurora B. Dev Cell 11, 741–750.

Dai J, Sultan S, Taylor SS, Higgins JM (2005). The kinase haspin is required for mitotic histone H3 Thr 3 phosphorylation and normal metaphase chromosome alignment. Genes Dev 19, 472–488.

De Antoni A, Maffini S, Knapp S, Musacchio A, Santaguida S (2012). A small-molecule inhibitor of Haspin alters the kinetochore functions of Aurora B. J Cell Biol 199, 269–284.

Ditchfield C, Johnson VL, Tighe A, Ellston R, Haworth C, Johnson T, Mortlock A, Keen N, Taylor SS (2003). Aurora B couples chromosome alignment with anaphase by targeting BubR1, Mad2, and Cenp-E to kinetochores. J Cell Biol 161, 267–280.

Duncan FE, Chiang T, Schultz RM, Lampson MA (2009). Evidence that a defective spindle assembly checkpoint is not the primary cause of maternal age-associated aneuploidy in mouse eggs. Biol Reprod 81, 768–776.

Hached K, Xie SZ, Buffin E, Cladiere D, Rachez C, Sacras M, Sorger PK, Wassmann K (2011). Mps1 at kinetochores is essential for female mouse meiosis I. Development 138, 2261–2271.

Hassold T, Sherman S (2000). Down syndrome: genetic recombination and the origin of the extra chromosome 21. Clin Genet 57, 95–100.

Higgins JM (2003). Structure, function and evolution of haspin and haspin-related proteins, a distinctive group of eukaryotic protein kinases. Cell Mol Life Sci 60, 446–462.

Hiruma Y, Koch A, Dharadhar S, Joosten RP, Perrakis A (2016). Structural basis of reversine selectivity in inhibiting Mps1 more potently than aurora B kinase. Proteins 84, 1761–1766.

Holt JE, Lane SI, Jennings P, Garcia-Higuera I, Moreno S, Jones KT (2012). APC(FZR1) prevents nondisjunction in mouse oocytes by controlling meiotic spindle assembly timing. Mol Biol Cell 23, 3970–3981.

Homer HA, McDougall A, Levasseur M, Murdoch AP, Herbert M (2005). Mad2 is required for inhibiting securin and cyclin B degradation following spindle depolymerisation in meiosis I mouse oocytes. Reproduction 130, 829–843.

Hunt PA, Hassold TJ (2002). Sex matters in meiosis. Science 296, 2181–2183.

Jacobs PA (1992). The chromosome complement of human gametes. Oxf Rev Reprod Biol 14, 47–72.

Kang H, Park YS, Cho DH, Kim JS, Oh JS (2015). Dynamics of histone H3 phosphorylation at threonine 3 during meiotic maturation in mouse oocytes. Biochem Biophys Res Commun 458, 280–286.

Kelly AE, Ghenoiu C, Xue JZ, Zierhut C, Kimura H, Funabiki H (2010). Survivin reads phosphorylated histone H3 threonine 3 to activate the mitotic kinase Aurora B. Science 330, 235–239.

Kimmins S, Crosio C, Kotaja N, Hirayama J, Monaco L, Hoog C, van Duin M, Gossen JA, Sassone-Corsi P (2007). Differential functions of the Aurora-B and Aurora-C kinases in mammalian spermatogenesis. Mol Endocrinol 21, 726–739.

Kitajima TS, Ohsugi M, Ellenberg J (2011). Complete kinetochore tracking reveals error-prone homologous chromosome biorientation in mammalian oocytes. Cell 146, 568–581.

Kuliev A, Zlatopolsky Z, Kirillova I, Spivakova J, Cieslak Janzen J (2011). Meiosis errors in over 20,000 oocytes studied in the practice of preimplantation aneuploidy testing. Reprod Biomed Online 22, 2–8.

Lane SI, Chang HY, Jennings PC, Jones KT (2010). The Aurora kinase inhibitor ZM447439 accelerates first meiosis in mouse oocytes by overriding the spindle assembly checkpoint. Reproduction 140, 521–530.

Lane SI, Jones KT (2014). Non-canonical function of spindle assembly checkpoint proteins after APC activation reduces aneuploidy in mouse oocytes. Nat Commun 5, 3444.

Lin BW, Wang YC, Chang-Liao PY, Lin YJ, Yang ST, Tsou JH, Chang KC, Liu YW, Tseng JT, Lee CT, *et al.* (2014). Overexpression of Aurora-C interferes with the spindle checkpoint by promoting the degradation of Aurora-B. Cell Death Dis 5, e1106.

Marquez C, Cohen J, Munne S (1998). Chromosome identification in human oocytes and polar bodies by spectral karyotyping. Cytogenet Cell Genet 81, 254–258.

McGuinness BE, Anger M, Kouznetsova A, Gil-Bernabe AM, Helmhart W, Kudo NR, Wuensche A, Taylor S, Hoog C, Novak B, Nasmyth K (2009). Regulation of APC/C activity in oocytes by a Bub1-dependent spindle assembly checkpoint. Curr Biol 19, 369–380.

Nguyen AL, Gentilello AS, Balboula AZ, Shrivastava V, Ohring J, Schindler K (2014). Phosphorylation of threonine 3 on histone H3 by haspin kinase is required for meiosis I in mouse oocytes. J Cell Sci 127, 5066–5078.

Niault T, Hached K, Sotillo R, Sorger PK, Maro B, Benezra R, Wassmann K (2007). Changing Mad2 levels affects chromosome segregation and spindle assembly checkpoint control in female mouse meiosis I. PLoS One 2, e1165.

Rattani A, Wolna M, Ploquin M, Helmhart W, Morrone S, Mayer B, Godwin J, Xu W, Stemmann O, Pendas A, Nasmyth K (2013). Sgol2 provides a regulatory platform that coordinates essential cell cycle processes during meiosis I in oocytes. Elife 2, e01133.

Santaguida S, Tighe A, D'Alise AM, Taylor SS, Musacchio A (2010). Dissecting the role of MPS1 in chromosome biorientation and the spindle checkpoint through the small molecule inhibitor reversine. J Cell Biol 190, 73–87.

Santaguida S, Vernieri C, Villa F, Ciliberto A, Musacchio A (2011). Evidence that Aurora B is implicated in spindle checkpoint signalling independently of error correction. EMBO J 30, 1508–1519.

Sasai K, Katayama H, Hawke DH, Sen S (2016). Aurora-C interactions with Survivin and INCENP reveal shared and distinct features compared with aurora-b chromosome passenger protein complex. PLoS One 11, e0157305.

Sasai K, Katayama H, Stenoien DL, Fujii S, Honda R, Kimura M, Okano Y, Tatsuka M, Suzuki F, Nigg EA, *et al*. (2004). Aurora-C kinase is a novel chromosomal passenger protein that can complement Aurora-B kinase function in mitotic cells. Cell Motil Cytoskeleton 59, 249–263.

Schindler K, Davydenko O, Fram B, Lampson MA, Schultz RM (2012). Maternally recruited Aurora C kinase is more stable than Aurora B to support mouse oocyte maturation and early development. Proc Natl Acad Sci USA 109, E2215–E2222.

Sharif B, Na J, Lykke-Hartmann K, McLaughlin SH, Laue E, Glover DM, Zernicka-Goetz M (2010). The chromosome passenger complex is required for fidelity of chromosome transmission and cytokinesis in meiosis of mouse oocytes. J Cell Sci 123, 4292–4300.

Slattery SD, Mancini MA, Brinkley BR, Hall RM (2009). Aurora-C kinase supports mitotic progression in the absence of Aurora-B. Cell Cycle 8, 2984–2994.

Stein P, Schindler K (2011). Mouse oocyte microinjection, maturation and ploidy assessment. J Vis Exp 53, 2851.

Tanaka H, Yoshimura Y, Nozaki M, Yomogida K, Tsuchida J, Tosaka Y, Habu T, Nakanishi T, Okada M, Nojima H, Nishimune Y (1999). Identification and characterization of a haploid germ cell-specific nuclear protein kinase (Haspin) in spermatid nuclei and its effects on somatic cells. J Biol Chem 274, 17049–17057.

Tseng TC, Chen SH, Hsu YP, Tang TK (1998). Protein kinase profile of sperm and eggs: cloning and characterization of two novel testis-specific protein kinases (AIE1, AIE2) related to yeast and fly chromosome segregation regulators. DNA Cell Biol 17, 823–833.

Vigneron S, Prieto S, Bernis C, Labbe JC, Castro A, Lorca T (2004). Kinetochore localization of spindle checkpoint proteins: who controls whom? Mol Biol Cell 15, 4584–4596.

Volarcik K, Sheean L, Goldfarb J, Woods L, Abdul-Karim FW, Hunt P (1998). The meiotic competence of in-vitro matured human oocytes is influenced by donor age: evidence that folliculogenesis is compromised in the reproductively aged ovary. Hum Reprod 13, 154–160.

Wang F, Dai J, Daum JR, Niedzialkowska E, Banerjee B, Stukenberg PT, Gorbsky GJ, Higgins JM (2010). Histone H3 Thr-3 phosphorylation by Haspin positions Aurora B at centromeres in mitosis. Science 330, 231–235.

Wang F, Ulyanova NP, Daum JR, Patnaik D, Kateneva AV, Gorbsky GJ, Higgins JM (2012). Haspin inhibitors reveal centromeric functions of Aurora B in chromosome segregation. J Cell Biol 199, 251–268.

Wang Q, Wei H, Du J, Cao Y, Zhang N, Liu X, Liu X, Chen D, Ma W (2016). H3 Thr3 phosphorylation is crucial for meiotic resumption and anaphase onset in oocyte meiosis. Cell Cycle 15, 213–224.

Wassmann K, Niault T, Maro B (2003). Metaphase I arrest upon activation of the Mad2-dependent spindle checkpoint in mouse oocytes. Curr Biol 13, 1596–1608.

World Health Organization. Programme of Maternal and Child Health and Family Planning Unit (1991). Infertility: a tabulation of available data on prevalence of primary and secondary infertility. Available at http://apps.who.int/iris/handle/10665/59769 (accessed 1 November 2016).

Yamagishi Y, Honda T, Tanno Y, Watanabe Y (2010). Two histone marks establish the inner centromere and chromosome bi-orientation. Science 330, 239–243.

Yanai A, Arama E, Kilfin G, Motro B (1997). ayk1, a novel mammalian gene related to Drosophila aurora centrosome separation kinase, is specifically expressed during meiosis. Oncogene 14, 2943–2950.

Yoshida S, Kaido M, Kitajima TS (2015). Inherent instability of correct kinetochore-microtubule attachments during meiosis I in oocytes. Dev Cell 33, 589–602.